Computers, Materials & Continua CMC, vol.62, no.1, pp.309-319, 2020

Image Interpolation via Gaussian-Sinc Interpolators with Partition of Unity

Gang Xu[1, *], Ran Ling[1], Lishan Deng[1], Qing Wu[1] and Weiyin Ma[2]

Abstract: In this paper, we propose a novel image interpolation method by using Gaussian-Sinc automatic interpolators with partition of unity property. A comprehensive comparison is made with classical image interpolation methods, such as the bicubic interpolation, Lanczos interpolation, cubic Schaum interpolation, cubic B-spline interpolation and cubic Moms interpolation. The experimental results show the effectiveness of the improved image interpolation method via some image quality metrics such as PSNR and SSIM.

Keywords: Image interpolation method, Gaussian-Sinc function, partition of unity property.

1 Introduction

Image interpolation is an important topic in the field of image processing and is the key technique for image super-resolution. Many kinds of analytic functions have been employed as image interpolation tools [Gao, Zhang, Zhang et al. (2008); Zhou, Pan, Wang et al. (2017)], including the representative approaches based on bicubic polynomial [Lin, Sheu, Chiang et al. (2008); Keys (2003)], Sinc function [Turkowski (1990)], and so on. One of the main interests is that they are interpolating, however, most of them have a worse approximation property compared with o-Moms [Blu, Thcvenaz and Unser (2001)] and B-splines [Unser, Aldroubi and Eden (1993)].

Recently, Sinc-function has been the holy grail of image interpolation. However, it has two drawbacks: firstly, it only can achieve an approximated interpolation; secondly, it decays slowly and ringing-associated effects may be spread out. In order to improve the performance of image interpolation with Sinc-function, in this paper, we propose a novel image interpolation technique by using the Gaussian-Sinc interpolation function. Gaussian-Sinc functions not only has automatic-interpolating property, but also satisfy partition of unity and has local support [Zhang (2012); Zhang and Ma (2011)]. Compared with conventional image interpolation tools (such as cubic spline interpolation, Lanczos interpolation, Schaum interpolation, cubic-B spline interpolation, Moms interpolation), the proposed image interpolation method has better performance in terms of PSNR and SSIM as illustrated in a large number of experimental results.

The rest of paper is organized as follows. In Section 2, a review of related image

[1] School of Computer Science and Technology, Hangzhou Dianzi University, Hangzhou, China.

[2] Department of Mechanical and Biomedical Engineering, City University of Hong Kong, Hong Kong.

[*] Corresponding Author: Gang Xu. Email: gxu@hdu.edu.cn.

interpolation is presented. In Section 3, the definition and properties of Gaussian-Sinc functions will be introduced. The image interpolation framework via Gaussian-Sinc functions is introduced in Section 4. Section 5 presents the experimental results, and the comparisons with traditional interpolators are shown via several examples. Section 6 concludes the paper with a summary and some future research topics.

2 Related work

Image interpolation has been widely studied for decades, in order to achieve more perfect interpolation effect, the image interpolation analytic functions have been employed as image interpolation tools. Bicubic polynomial interpolation method [Lin, Sheu, Chiang et al. (2008); Keys (2003)] is one of the most popular image interpolation approaches [Chen, Huang and Luo (2011)]. Lanczos interpolation [Turkowski (1990)] is based on sinc function, which is the best compromise in terms of reduction of aliasing, sharpness, and minimal ringing for decimation and interpolation of two-dimensional and three-dimensional data. However, Lanczos interpolator does not have the partition of unity (POU) property [Turkowski (1990)]. As shown in Thévenaz et al. [Thévenaz, Blu and Unser (2000)], the POU property is a key issue in image processing because the spectrum of images is very often concentrated towards low frequencies, and it is equivalent to impose that its Fourier transform satisfies some sort of interpolation property in the Fourier domain. Cubic B-spline also is employed in image interpolation [Unser, Aldroubi and Eden (1993)], but it is not an interpolator, and a linear system must be solved to ensure the function goes through the data points exactly [Unser (1999)]. The exponential spline is also used in image interpolation as introduced in Kirshner et al. [Kirshner and Porat (2009)]. Moms (Maximal Order of Minimal Support) function [Blu, Thevenaz and Unser (2001)] used for image interpolation, is the weighted sum of a B-spline and its derivatives. As B-splines, they also do not have interpolation property. Like the optimal-Moms, Schaum functions [Schaum (1993)] are the pseudo-Lagrangian basis functions proposed by Schaum, which can be also represented as a weighted sum of B-splines and of their even-order derivatives [Thévenaz, Blu and Unser (2000)].

In recent years, some state-of-the-art image interpolation approaches became popular in the field of image processing. An edge-directed interpolation is proposed to estimate local covariance coefficients from a low resolution image and adapt the interpolation at a higher resolution based on the geometric duality between their covariance [Li and Orchard (2001)]. In Li [Li (2008)], a patch-based image interpolation method is proposed as an alternate to the projection onto two convex sets of observation data and the other defined by a sparsity-based nonlocal prior. A single frame super resolution algorithm is proposed in Hung et al. [Hung and Siu (2015)] by using a finite impulse response.

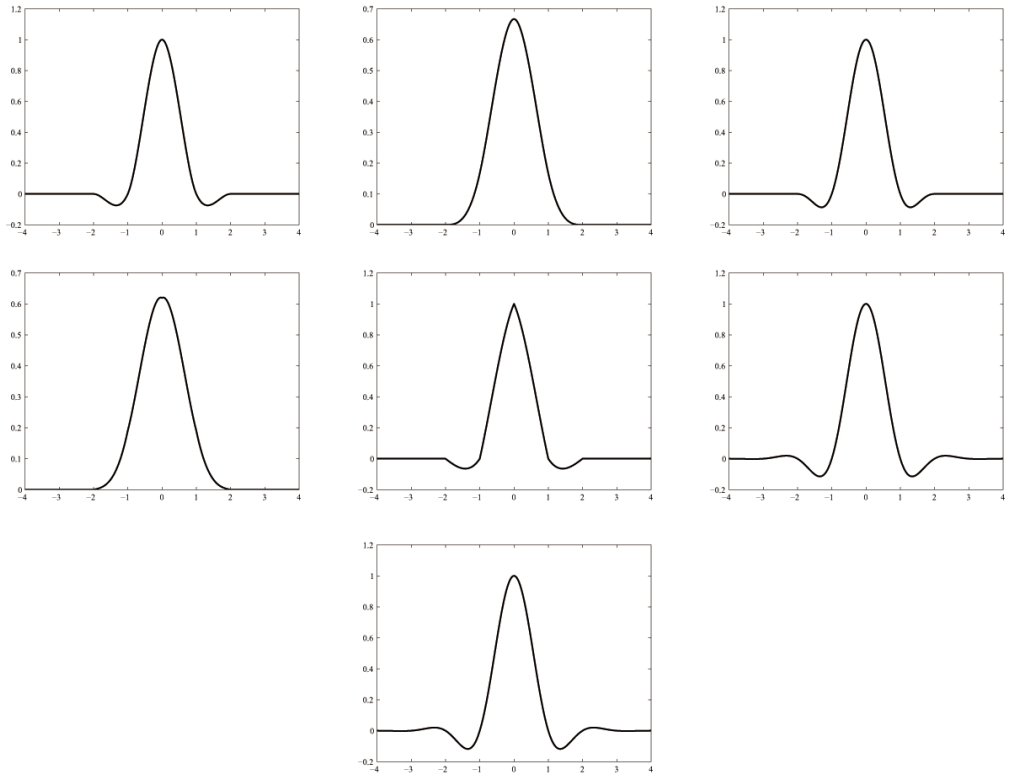

Figure 1: Comparison of basic functions used in image interpolation

3 Gaussian-Sinc interpolators and properties

In this section, we will present the definition and property of Gaussian-Sinc interpolators. Gaussian-Sinc interpolation kernel function is derived from Gaussian function and Sinc unction, and it is defined as follows:

$$\phi(x,a)=\begin{cases}\dfrac{\sin(\pi x)}{\pi x}e^{-ax^2}, & x\neq 0;\\ 1, & x=0.\end{cases}$$

The parameter a is a positive constant, which affects the shape and local support of the kernel function. This new interpolator has several interesting properties, such as symmetry, C^{∞} continuity, local support, almost partition of unity (POU), almost linear precision. Gaussian-Sinc basis function can achieve automatic interpolation for the given data points without solving linear systems. That is, given a set of data points P_i , the parametric curve $P(t)=\sum P_i\phi(t-i,a)$ interpolates the points P_i:

$$\phi_i(x,a):=\phi(x-i,a)=\begin{cases}1, & x=i;\\ 0, & x=\cdots,i-1,i+1,\cdots\end{cases}$$

Remark 1. The almost partition of unity (POU) means that the Gaussian-Sinc interpolation functions do not provide sufficiently high accuracy of POU, for example, when a=1/3, the maximum error of POU is about 0.0003.

Gaussian-Sinc interpolator can be improved to achieve partition of unity as shown in the following formula:

$$\Phi(x,a,b,\lambda)=\phi(x,a)+\lambda x\sin(\pi x)e^{-bx^2},$$

where a and b are constants, λ is a constant which depends on a and b as defined in the following,

$$\lambda=\frac{2}{\sqrt{\pi}}\left(1-\frac{2}{\sqrt{\pi}}\int_0^{\frac{2}{2\sqrt{a}}}e^{-t^2}dt\right)b^{\frac{3}{2}}e^{\frac{\pi^2}{4b}}. \tag{1}$$

The interpolator defined in (1) is called improved Gaussian-Sinc interpolating function. Fig. 1 shows the classical basis functions for image interpolation, the Gaussian-Sinc basis function (Fig. 1 (f)), and the improved Gaussian-Sinc interpolating function (Fig. 1 (g)).

4 Image interpolation based on Gaussian-Sinc interpolators

In traditional image interpolation method [Thévenaz, Blu and Unser (2000)], we can define the interpolation function $f(X)$ at parameters X in the following way:

$$\begin{aligned} &f(X)=\sum_{k\in Z^q}f_k\bullet\phi_{\text{int}}(X-K),\\ &\forall X=(x_1,x_2,...,x_q)\in R^q, \end{aligned} \tag{2}$$

in which x_k is the sampling points at integer coordinates $K=(k_1,k_2,...k_q)\in Z^q$,the weights of sampling points f_k is up to $\phi_{\text{int}}(X-K)$. In order to satisfy the requirement of interpolation precision, the kernel function ϕ_{int} must possess the precise interpolation property, that is, $\phi_{\text{int}}=0$ at any integer point except the origin, and $\phi_{\text{int}}=1$ at the origin. However, the selection of interpolation kernel function is limited by this requirement.

A general interpolation function $f(X)$ can be written as follows [Thévenaz, Blu and Unser (2000)] to select flexible interpolating basis function and improve the interpolating precision:

$$\begin{aligned} &f(X)=\sum_{k\in Z^q}c_k\bullet\phi_{\text{int}}(X-K),\\ &\forall X=(x_1,x_2,...,x_q)\in R^q, \end{aligned} \tag{3}$$

The main difference between formula (2) and (3) is that the coefficient c_k instead of the sample points f_k in the interpolation formula (2), which expands the selecting range of the interpolation basis function. At the same time, formula (3) introduces a new interpolation step, thus, this interpolation method is divided into two steps: firstly, compute the interpolation coefficient c_k according to the sample points f_k; Secondly, compute the function value at unknown parameter points by using the values of c_k.

It is obvious that the larger value of a, the smaller value of $|\phi(x,a)|$. That is, the local support of the kernel function is smaller. However, when a is larger, the interpolation precision is lower. Meanwhile, the improved interpolation basis function has the almost same local support. On the other hand, a kernel function has smaller local support, it has the better local property. Local property can guarantee the local adjustment of the interpolation function without affecting other data points. In this way, it ensures the accuracy of the interpolation and can reduce effectively the effect of artifacts. At the same time, it can also reduce the complexity of the calculation to improve the computational efficiency. In order to achieve balance between the interpolation accuracy and the local support of the kernel function, in this paper, we set the parameters $a=\frac{1}{3}$, $b=\frac{1}{2}$ and the corresponding optimal λ for image interpolation.

5 Experimental results and comparison

In this section, some experimental results and comparison with traditional methods will be presented to show the effectiveness of the proposed methods.

Peak-signal-to-noise ratio (PSNR for short) is an important and objective measurement to evaluate image quality [Wang, Bovik, Sheikh et al. (2004)], and its definition can be written as follows:

$$PSNR = 10 \times \log_{10} \frac{255^2}{MSE}, \tag{4}$$

$$MSE = \frac{1}{M \times N} \sum_{i=1}^{N} \sum_{j=1}^{M} \left(f_{ij} - f_{ij}^{'} \right), \tag{5}$$

in which M and N are length and width of an image respectively, f_{ij} and $f_{ij}^{'}$ are the pixel values of the original image and the pixel values of the reconstructed image. On the other hand, the structural-similarity-index-measure (SSIM for short) is used as another evaluation measurement for image interpolation [Wang, Bovik, Sheikh et al. (2004)]. Big value of SSIM (the maximum is 1) illustrates that the structure of the two images is more similar and the image interpolation method is better.

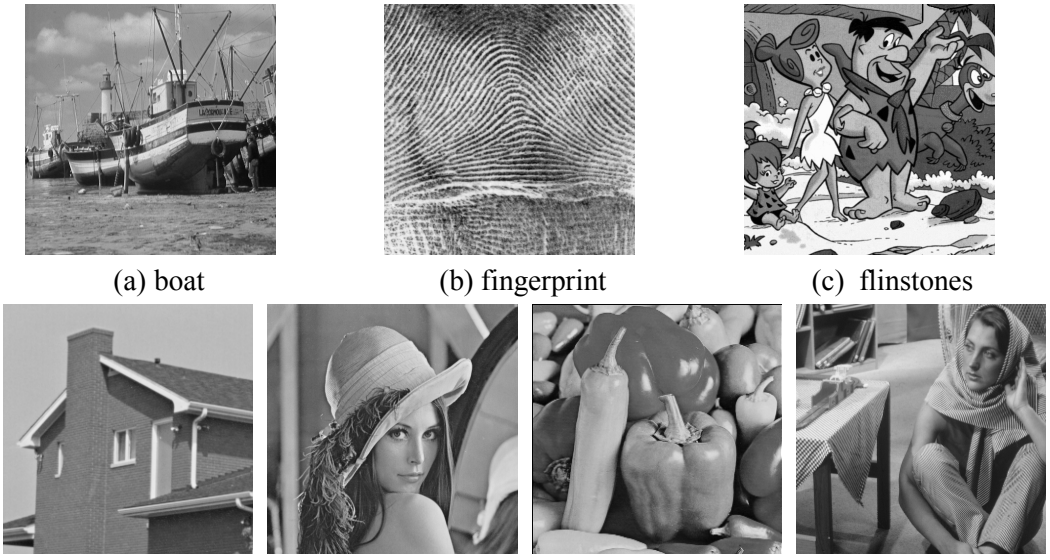

(a) boat (b) fingerprint (c) flinstones

(d) house (e) lena (f) peppers (g) barbara

Figure 2: The original images

In this paper, seven classical pictures used in image processing are tested as experimental examples, and the original images are shown in Fig. 2. Firstly, sample the original images as low resolution ones, then use the kernel function mentioned in this paper as the image interpolation basic function to reconstruct the images from low resolution images. Finally, the value of PSNR and SSIM between the original images and reconstruction images are computed to compare the various different image interpolation methods as shown in Tab. 1, in which GS I and GS II denotes the Gaussian-Sinc interpolation method and the improved Gaussian-Sinc interpolation method respectively. We can find that the improved Gaussian-Sinc function has the best performance in terms of PSNR and SSIM. Fig. 3 and Fig. 4 show the zoom-in interpolation results for two regions of interest in Peppers image with different interpolation method.

Experiment II In this experiment, the original high resolution image is sampled by 9:1 (length and width by scaling 3 times respectively) to obtain the corresponding low-resolution images. Then the Lanczos function, cubic B-spline, cubic Moms function, Gaussian-Sinc function and the improved Gaussian-Sinc function are used as the interpolating kernel function in the image interpolation experiment. Finally, we evaluate the value of PSNR and SSIM between the original images and reconstruction images, which are listed in Tab. 2, in which GS I and GS II denotes the Gaussian-Sinc interpolation method and the improved Gaussian-Sinc interpolation method respectively.

Table 1: PSNR and SSIM of different image interpolation with scale factor S=2

	PSNR (dB)				
	Bicubic	Lanczos	Schaum3	GS I	GS II
boat	30.1023	30.1307	29.8884	30.7862	**31.2974**
fingerprint	30.6631	30.7825	30.3850	31.8272	**32.2830**
flinstones	26.7949	26.8804	26.5283	27.9077	**28.3472**
house	32.8947	32.9244	32.6601	33.6582	**34.0724**
lena	34.2893	34.3372	34.0389	35.9235	**35.6486**
peppers	27.3056	27.3567	27.2603	28.5387	**28.5571**
barbara	25.4902	25.4870	25.2794	26.3090	**26.4213**
			SSIM		
	Bicubic	Lanczos	Schaum3	GS I	GS II
boat	0.8600	0.8603	0.8535	0.8738	**0.8840**
fingerprint	0.9536	0.9546	0.9501	0.9689	**0.9793**
flinstones	0.8725	0.8729	0.8660	0.8884	**0.8987**
house	0.8969	0.8965	0.8916	0.9075	**0.9146**
lena	0.9225	0.9227	0.9185	0.9311	**0.9356**
peppers	0.9197	0.9196	0.9158	0.9286	**0.9317**
barbara	0.8092	0.8096	0.7964	0.8179	**0.8220**

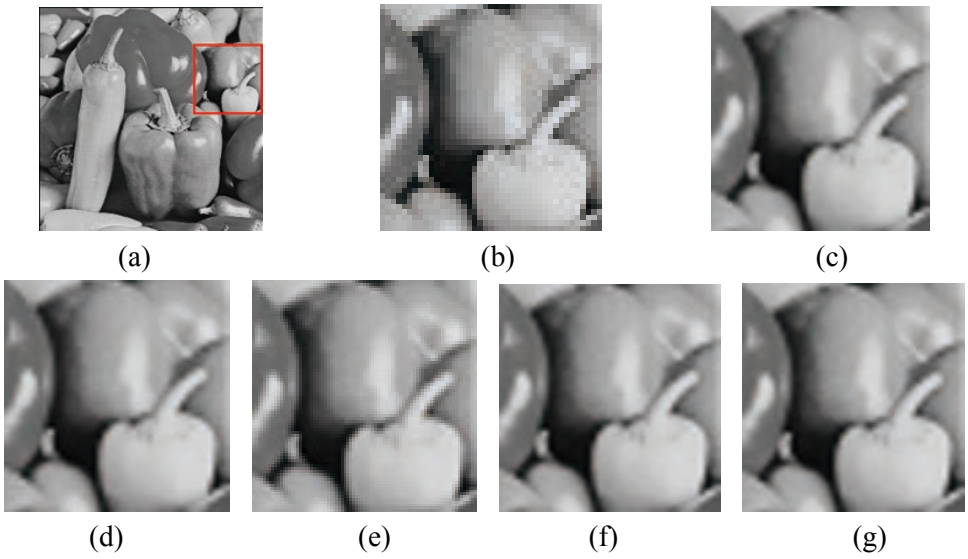

Figure 3: Image interpolation for "Peppers": (a) original image, (b) the low-resolution Peppers image, (c) Bicubic interpolation, (d) Lanczos interpolation, (e) Cubic Schaum interpolation, (f) Gaussian-Sinc interpolation, (g) improved Gaussian-Sinc interpolation

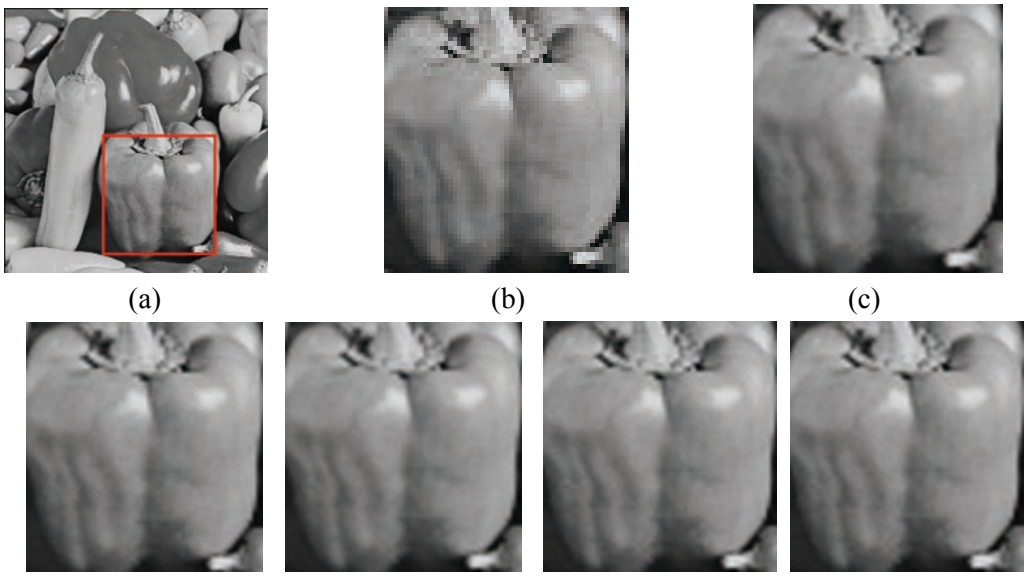

Figure 4: Image interpolation for a region of interest on image "Peppers": (a) the original Peppers image, (b) the low-resolution Peppers image, (c) Bicubic interpolation, (d) Lanczos interpolation, (e) Cubic Schaum interpolation, (f) Gaussian-Sinc interpolation, (g) improved Gaussian-Sinc interpolation

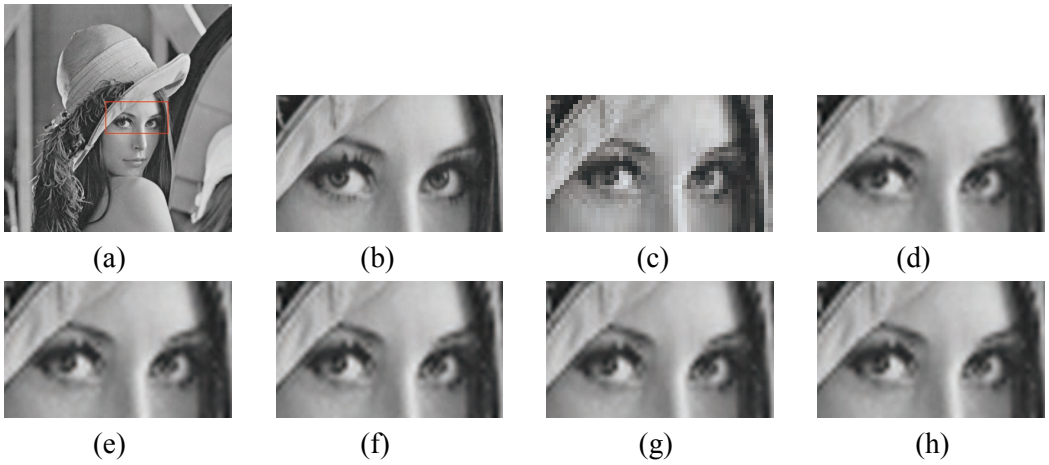

Figure 5: Image interpolation for image "Lena": (a) the original image, (b) the original region of interest, (c) the low-resolution region of interest, (d) Lanczos interpolation, (e) Cubic B-spline interpolation, (f) Cubic Moms-interpolation, (g) Gaussian-Sinc interpolation, (h) improved Gaussian-Sinc interpolation

Table 2: PSNR and SSIM of different interpolation methods with scale factor S=3

			PSNR (dB)		
	Lanczos	Bspline3	O-Moms3	GS I	GS II
boat	27.7993	27.8710	27.7386	28.4707	**28.9584**
fingerprint	27.6932	27.7474	27.6426	28.7345	**28.9480**
flinstones	23.8141	23.8518	23.7757	24.8643	**25.8654**
house	28.9583	29.0108	28.9023	29.1923	**29.5847**
lena	31.8183	31.8848	31.7570	32.3493	**32.9459**
peppers	22.3891	22.4290	22.3619	23.4542	**23.6751**
barbara	24.5509	24.6505	24.4864	25.3771	**25.8532**
			SSIM		
	Lanczos	Bspline3	O-Moms3	GS I	GS II
boat	0.8232	0.8249	0.8195	0.8393	**0.8428**
fingerprint	0.9122	0.9118	0.9109	0.9213	**0.9235**
flinstones	0.8157	0.8174	0.8082	0.8240	**0.8355**
house	0.8317	0.8334	0.8277	0.8482	**0.8498**
lena	0.8994	0.9007	0.8974	0.9129	**0.9177**
peppers	0.8477	0.8500	0.8433	0.8575	**0.8645**
barbara	0.7413	0.7435	0.7389	0.7443	**0.7574**

The improved Gaussian-Sinc interpolator also can obtain the best interpolation results. Fig. 5 and Fig. 6 present the zoom-in interpolation results for the two regions of interest image "Lena" with different interpolation methods.

We have performed the above evaluation for a complicated database, and similar results are obtained. In terms of computing complexity, Tab. 3 shows the computing costs of each method. From Tab. 3, we can find that the proposed method has a comparable and similar computing complexity with the previous approaches.

6 Conclusion

In this paper, we propose a new image interpolation method based on Gaussian Sinc interpolating functions. By comparing with the classical image interpolation methods, including Bi-cubic spline interpolation, Lanczos interpolation, cubic Schaum interpolation, cubic B-spline interpolation and cubic Moms interpolation, we can find that the proposed image interpolation method can achieve better performance on the PSNR and SSIM metrics. In the future, we will extend the present work to video interpolation problems.

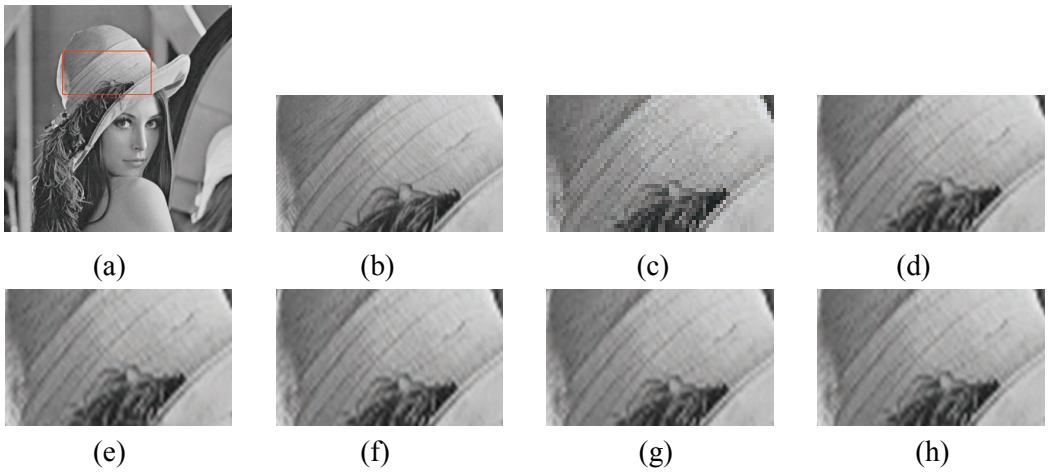

Figure 6: Image interpolation for image "Lena": (a) the original image, (b) the original region of interest, (c) the low-resolution region of interest, (d) Lanczos interpolation, (e) Cubic B-spline interpolation, (f) Cubic Moms-interpolation, (g) Gaussian-Sinc interpolation, (h) improved Gaussian-Sinc interpolation

Table 3: Computing costs of different interpolation methods (in seconds)

	Experiment I					Experiment II				
	Bicubic	Lanczos	Schum3	GSinc	ImpSinc	Lanczos	Bspline3	O-Moms3	GSinc	ImpSinc
boat	0.047	0.047	0.047	0.062	0.062	0.047	0.047	0.046	0.061	0.063
fingerprint	0.047	0.047	0.046	0.061	0.063	0.047	0.048	0.047	0.063	0.062
flinstones	0.046	0.047	0.047	0.062	0.063	0.047	0.047	0.047	0.062	0.062
house	0.016	0.016	0.015	0.016	0.016	0.016	0.015	0.016	0.016	0.015
lena	0.047	0.047	0.047	0.062	0.062	0.047	0.047	0.047	0.062	0.062
peppers	0.015	0.016	0.016	0.016	0.016	0.016	0.016	0.015	0.016	0.016
barbara	0.048	0.047	0.047	0.062	0.063	0.047	0.047	0.048	0.062	0.063

Acknowledgement: The authors thank the reviewers for their valuable comments which have helped to improve this paper. This research was supported by the National Nature Science Foundation of China under Grant Nos. 61772163, 61761136010, Zhejiang Provincial Natural Science Foundation of China under Grant No. LR16F020003, and Zhejiang Provincial Science and Technology Program in China (2018C01030). Scientific Research Fund of Hunan Provincial Education Department (No. 15A110).

References

Blu, T.; Thcvenaz, P.; Unser, M. (2001): Moms: maximal-order interpolation of minimal support. *IEEE Transactions on Image Processing: A Publication of the IEEE Signal Processing Society*, vol. 10, no. 7, pp. 1069.

Chen, S. L.; Huang, H. Y.; Luo, C. H. (2011): A low-cost high-quality adaptive scalar for real-time multimedia applications. *IEEE Transactions on Circuits and Systems for Video Technology*, vol. 21, no. 11, pp. 1600-1611.

Gao, S. S.; Zhang, C. M.; Zhang, Y, F.; Zhou, Y. F. (2008): Medical image zooming algorithm based on bivariate rational interpolation. *International Symposium on Visual Computing*, pp. 672-681.

Hung, K.; Siu, W. (2015): Single-image super-resolution using iterative Wiener filter based on nonlocal means. *Signal Processing-image Communication*, vol. 39, pp. 26-45.

Kirshner, H.; Porat, M. (2009): On the role of exponential splines in image interpolation. *IEEE Transactions on Image Processing*, vol. 18, no. 10, pp. 2198-2208.

Keys, R. (2003): Cubic convolution interpolation for digital image processing. *IEEE Transactions on Acoustics, Speech, and Signal Processing*, vol. 29, no. 6, pp. 1153-1160.

Lin, C. C.; Sheu, M. H.; Chiang, H. K.; Liaw, C.; Wu, Z. C. (2008): The efficient VLSI design of bi-cubic convolution interpolation for digital image processing. *IEEE International Symposium on Circuits and Systems*, pp. 480-483.

Li, X. (2008): Patch-based image interpolation: algorithms and applications. *International Workshop on Local and Non-Local Approximation in Image Processing*, pp. 1-6.

Li, X.; Orchard, M. T. (2001): New edge-directed interpolation. *IEEE Transactions on Image Process*, vol. 10, no. 10, pp. 1521-1527.

Schaum, A. (1993): Theory and design of local interpolators. *CVGIP: Graphical Models and Image Processing*, vol. 55, no. 6, pp. 464-481.

Turkowski, K. (1990): Filters for common resampling tasks. *Graphics Gems*.

Thévenaz, P.; Blu, T.; Unser, M. (2000): Interpolation revisited. *IEEE Transactions on Medical Imaging*, vol. 19, no. 7, pp. 739-758.

Thévenaz, P.; Blu, T.; Unser, M. (2000): Image interpolation and resampling. *Handbook of Medical Imaging*, vol. 87, no. 3, pp. 393-420.

Unser, M. (1999): Splines: a perfect fit for signal and image processing. *IEEE Signal Processing Magazine*, vol. 16, no. 6, pp. 22-38.

Unser, M.; Aldroubi, A.; Eden, M. (1993): B-spline signal processing. I. Theory. *IEEE Transactions on Signal Processing*, vol. 41, no. 2, pp. 821-833.

Wang, Z.; Bovik, A. C.; Sheikh, H. R.; Simoncelli, E. P. (2004): Image quality assessment: from error visibility to structural similarity. *IEEE Transactions on Image Processing*, vol. 13, no. 4, pp. 600-612.

Zhang, R. (2012): Curve and surface reconstruction based on a set of improved interpolatory basis functions. *Computer Aided Design*, vol. 44, no. 8, pp. 749-756.

Zhang, R. J.; Ma, W. (2011): An efficient scheme for curve and surface construction based on a set of interpolatory basis functions. *ACM Transactions on Graphics*, vol. 30, no. 2, pp. 1-11.

Zhou, Y. F.; Pan, X.; Wang, W. P.; Yin, Y. L.; Zhang, C. M. (2017): Superpixels by bilateral geodesic distance. *IEEE Transaction on Circuits and System for Video Technology*, vol. 27, no. 11, pp. 2281-2293.